Surface-bounded Atmosphere of Europa

V. I. Shematovich

Institute of Astronomy, Russian Academy of Sciences,
48 Pyatnistkaya street, Moscow, 119017 Russia
(e-mail: shematov@inasan.rssi.ru)

R. E. Johnson

Engineering Physics Program and Astronomy Department,
University of Virginia, Thornton Hall B103, Charlottesville, VA 22903

J. F. Cooper

Raytheon Technical Services Company LLC, SSDOO Project, Code 632,
NASA Goddard Space Flight Center, Greenbelt, MD 20771, USA

M. C. Wong

Jet Propulsion Laboratory, 4800 Oak Grove Drive, Pasadena CA, 91109

Pages: 53
Tables: 4
Figures: 6

Proposed Running Head: Surface-bounded Atmosphere of Europa

Editorial correspondence to:

Dr. Valery I. Shematovich

Institute of Astronomy, Russian Academy of Sciences
48 Pyatnistkaya street
Moscow, 119017 Russian Federation
Phone: (7-095) 9510730
Fax: (7-095) 2302081
E-mail: shematov@inasan.rssi.ru

ABSTRACT

A collisional Monte Carlo model of Europa's atmosphere is described in which the sublimation and sputtering sources of H_2O molecules and their molecular fragments are accounted for as well as the radiolytically produced O_2. Dissociation and ionization of H_2O and O_2 by magnetospheric electron, solar UV-photon and photo-electron impact, and collisional ejection from the atmosphere by the low-energy plasma are taken into account. Reactions with the surface are discussed, but only adsorption and atomic oxygen recombination are included in this model. The size of the surface-bounded oxygen atmosphere of Europa is primarily determined by a balance between atmospheric sources from irradiation of the satellite's icy surface by the high-energy magnetospheric charged particles and atmospheric losses from collisional ejection by the low-energy plasma, photo- and electron impact dissociation, and ionization and pick-up from the surface-bounded atmosphere. A range of sources rates for O_2 to H_2O are used with a larger oxygen-to-water ratio than suggested by laboratory measurements in order to account for differences in adsorption onto grains in the regolith. These calculations show that the atmospheric composition is determined by both the water and oxygen photochemistry in the near-surface region, escape of suprathermal oxygen and water into the Jovian system, and the exchange of radiolytic water products with the porous regolith. For the electron impact ionization rates used, pick-up ionization is the dominant oxygen loss process, whereas photo-dissociation and atmospheric sputtering are the dominant sources of neutral oxygen for Europa's neutral torus. Including desorption and loss of water enhances the supply of oxygen species to the neutral torus, but hydrogen produced by radiolysis is the dominant source of neutrals for Europa's torus in these models.

***Key words*:** Satellites: icy surfaces: sputtering; satellites: atmosphere; satellites: Europa

1. INTRODUCTION

The very tenuous O_2 atmosphere of Europa is an example of a surface-bounded or surface boundary layer atmosphere (Johnson 2002). It is produced from irradiation of Europa's exposed outer surface by solar ultraviolet photons and magnetospheric plasma. The O_2 atmosphere was observed indirectly using HST (Hall *et al.* 1995, 1998), the ionosphere was observed by Galileo (Kliore *et al.* 1997), and the neutral torus at Europa's jovicentric orbit was detected by Galileo (Lagg *et al.* 2003) and Cassini (Mauk *et al.* 2003). Being able to model the HST observations allows the unique and exciting possibility of being able to determine the rate of surface chemical modification on Europa from irradiation effects. This is important as irradiation is a dominant surface alteration process on outer solar system bodies (Johnson *et al.* 2003a) including those in the Kuiper Belt and the Oort cloud (Strazzulla *et al.* 2003). Oxidant production by irradiation is a potential astrobiological resource for life within Europa's putative subsurface ocean (Chyba 2000; Cooper et al. 2001), while also acting to limit survival of recognizable biomolecules at the accessible surface via destructive oxidation from surface and atmospheric species. Determination of surface chemical composition, both in-situ at the surface and remotely via atmospheric sampling from Europa orbit, and the search for biochemical signs of life will be important goals of the planned Jupiter Icy Moons Orbiter (JIMO) mission. Development of coupled models for the magnetospheric environment of Europa, surface chemistry driven by irradiation effects, and the structure and composition of the atmosphere arising from such effects are needed for planning future investigations of Europa.

The plasma interaction with the surface is the principal source of O_2 and the plasma interaction with the atmosphere is a principal loss process, therefore a large atmosphere does not accumulate (Johnson *et al.* 1982). Ip (1996) modeled the atmosphere using the sputtering rates estimated in Shi *et al.* (1995) and a simple model for the plasma interaction. More recently, Saur *et al.* (1998) carried out a more detailed description of the plasma interaction with the ionosphere to account for the change in energy and deflection of the flowing plasma. They used this along with a range of surface sputtering sources and an oversimplified, analytic model for an escaping-atmosphere in order to determine the column density and surface source rates implied by the HST observations of excited atomic O and to determine the electron densities in the ionosphere. In these models the atmosphere was assumed to be globally uniform. Although the atmosphere is not likely to be uniform, we describe here a model 1-D atmosphere and discuss the effect of having a non-uniform atmosphere in the summary.

Earlier we presented a collisional Monte Carlo model of Europa's atmosphere (Shematovich and Johnson, 2001) accounting for adsorption, thermalization and re-emission of condensed O_2. We used a 1-D Direct Simulation Monte Carlo (DSMC) method to model atmospheric thermal structure and the production rate of atomic O when the surface source is purely O_2 formed by radiolytic decomposition of ice. In that paper the oxygen loss was dominated by ionization from atmospheric irradiation by plasma electrons and subsequent sweeping away of the new ions by the corotating magnetic field of Jupiter's magnetosphere. However, the supply rate for oxygen to the neutral torus was dominated by photo-dissociation. That is also the case for the pure oxygen model described here, but the surface source rate given in that paper was over estimated and is corrected here. In this paper we further modify this model by including thermal and non-thermal sources of H_2O molecules and the production of water molecule fragments in the atmosphere.

2. PHYSICAL MODEL

2.1. Surface Source Rates

The H_2O surface source rates are chosen to explore the parameter space associated with sublimation and radiolytic sources based on measured yields and the ion flux data (Eviatar *et al.* 1985; Shi *et al.* 1995; Ip *et al.* 1998, Cooper *et al.* 2001). Estimates of the H_2O sputter source rates at Europa have varied from ~2×10^8 H_2O $cm^{-2}s^{-1}$ to ~ 2×10^{11} H_2O $cm^{-2}s^{-1}$ (Johnson *et al.* 2003a,b). The very large early estimates were due to large uncertainties in the sputtering yields. Since a considerable body of laboratory data has been accumulated (Johnson *et al.* 1998; 2003a,b) the present uncertainties in the estimates arise from limited knowledge of the energy spectrum of the incident plasma, particularly at the lower energies, variability in the plasma ion composition (Paranicas *et al.* 2002), and the importance of pick-up ion impact (Ip 1996). In addition, local increases of surface temperature (e.g., Johnson 1990), thin frost layers deposited on top of the crustal ice (Baragiola *et al.* 2003), and the presence of volatile species within the surface ice can all lead to enhanced sputtering rates. Conversely, the presence of hydrated species (McCord *et al*. 1999; Carlson *et al.* 1999) can reduce the effective yields relative to those for pure ice. Regolith porosity can both reduce yields for direct sputtering but perhaps also increase yields due to catalytic reactions at gas-solid interfaces of high surface area within regolith pores.

Under the assumption that the energetic particles measured by Voyager were predominantly oxygen ions, Shi *et al.* (1995) summarized the sputtering yields and plasma data and obtained globally averaged sputtering rates of 1.5×10^{11} H_2O $cm^{-2}s^{-1}$ for the energetic particles and 1.4×10^{9} H_2O $cm^{-2}s^{-1}$ for the low energy plasma ions. Ip (1996) and Eviatar *et al.* (1985) give comparable globally averaged source rates for the low energy plasma. In Shi *et al.* (1995) an enhancement for isotropic incidence of about a factor of 4 is included [recent modeling suggests a factor of 2.5 is more appropriate (Jurac *et al.* 2001))], and an enhancement for gyromotion of ~1.5 (Pospieszalska and Johnson 1989). Sticking to neighboring grains in the regolith reduces these rates. Since H_2O sticks with unit efficiency a reduction factor ~4 was shown to be appropriate (Johnson 1989; 1990). Therefore, these enhancements and reductions roughly cancel in determining the H_2O yields.

Whereas Voyager data indicated that protons were only about 15% of the low energy plasma (Bagenal 1994), the Galileo EPD (Energetic Particle Detector) measurements showed that the energetic ion flux (> 10keV) was dominated by protons. Therefore, the Shi *et al.* (1995) rates are likely to be high. Initial EPD data suggested $\sim1.7\times10^{9}$ H_2O $cm^{-2}s^{-1}$ (Ip *et al.* 1998; Cooper *et al.* 2001), whereas Paranicas *et al.* (2002) found $\sim8.0\times10^{9}$ H_2O $cm^{-2}s^{-1}$ using later EPD data with new corrections for cumulative radiation damage to detectors. They also indicated order of magnitude variations were possible due to variations in the ion flux and composition based on data from many Europa encounters. These estimates did not include the above-mentioned enhancement or reduction factors due to angular distributions, gyro-motion, and regolith porosity. Ip *et al.* (2000) estimated net total globally averaged sputtering rates of $\sim0.56\text{--}5.6\times10^{10}$ H_2O $cm^{-2}s^{-1}$ with the upper limit coming from their assumption of secondary sputtering by pickup ions from the atmosphere. Therefore, source rates ranging from $\sim (0.2 \text{ to } 20.)\times10^{10}$ H_2O $cm^{-2}s^{-1}$ have been suggested if the surface is water ice. However, these global averages are heavily weighted by the maximal irradiation intensities expected for magnetospheric ions incident on the trailing hemisphere, where the ice is observed to be mixed with hydrated compounds (e.g., salts, sulfuric acid) having relatively low sputtering yield compared to pure water ice, so the upper limits may be overestimates. In addition the potential corrections for surface temperature, gyro-motion effects, and diversion of magnetospheric plasma flow by ionospheric interactions need to be considered.

Based on the surface temperatures measured by Galileo (Spencer *et al.* 1999), the global average sublimation rate at a disk-averaged temperature of 106 K is small and comparable to the atmospheric contribution from micrometeoroid impact vaporization $\sim10^{7}$ H_2O $cm^{-2}s^{-1}$ from Cooper *et al.* (2001), if water molecules are present as ice. However, areas of the dayside equatorial regions can have temperatures up to 132 K, which gives a sublimation rate of 10^{11} $H_2O/cm^{-2}s^{-1}$. Any localized region sublimating at this rate would be rapidly depleted of volatiles in the absence of continually operating sources, so the global average is probably more representative. Freshly-deposited frosts or ice containing volatiles, and any localized sites of cryovolcanic activity releasing volatiles to the surface from subsurface regions, could undergo rapid sublimation, but comparison of Voyager and Galileo images for Europa over a twenty-year time span (Phillips et al. 2000) shows no evidence for frost or ejecta deposits from such activity at the resolution of several square kilometers for the entire imaged surface. Far greater spatial and temporal coverage for this search would be offered by the planned JIMO mission. Long term monitoring of atmospheric densities from earth-based telescopes might also reveal sudden bursts of such activity and is strongly encouraged.

The relative O_2/H_2O sputtering rate from ice has been shown to depend on the ice temperature and ion type and energy (e.g., Johnson 1990). The ratio used in earlier work was based on laboratory measurements at temperatures relevant to Europa's surface temperatures. This suggested a ratio of the order of ~ 0.1 to 0.2 (Johnson 1990; 1998). At the average Europa surface temperatures, Bar-Nun *et al.* (1985) found a larger ratio, ~0.5 for slow heavy ions, but Baragiola *et al.* (2003) also found ~0.2 for incident 100keV Ar^+ ions with larger ratios for incident O^+. These ratios apply to vapor deposited laboratory samples in which the surface porosities are often not known. When the porosity is large, as in an icy planetary regolith, and the sticking probability is high, the effective sputtering yields are reduced (e.g., Johnson 2002). Since H_2O sticks with unit efficiency but O_2 does not stick at Europa's temperatures, the effective O_2/H_2O ratio is increased significantly. In addition, O_2 produced at considerable depths by lightly ionizing energetic protons and electrons, the dominant carriers of the plasma energy, can slowly diffuse out, so that a relatively large O_2 source may be possible (Cooper *et al.* 2001). Moreover, the terrestrial measurements of air-snowpack interactions in Antarctica (Dominé and Shepson 2002) show that photolytic production of oxidants can increase by orders of magnitude due to two-phase (solid-gas) interactions on grains in sunlit snowpack ice.

As the properties and composition of Europa's surface and the plasma flux become better known, and as we improve our understanding of the sputtering and radiolysis of frozen molecular solids, these uncertainties will be reduced. We first re-evaluate the source rate for a pure O_2 atmosphere and obtain an O_2 source rate, constrained by the oxygen atmosphere observations, of $\sim 2.0\times10^9$ O_2 $cm^{-2}s^{-1}$. We use this and consider H_2O source rates ranging from $(0.2\text{-}2.)\times10^{10}$ H_2O $cm^{-2}s^{-1}$. In a few cases, large O_2 source rates are also considered. Although O and H are also directly sputtered from the surface (e.g., Bar-Nun *et al.* 1985; Kimmel *et al.*1995), the yields are not well measured but are expected to be small for fast, light ions. Therefore, we do not include these in the modeling presented here.

2.2. Energy Distributions

There are only a few measurements of the energy spectra for sputtered water molecules (e.g., Johnson 1990; 1998). As the sputtering of frozen molecular solids is dominated by solid state chemistry, referred to as radiolysis (e.g., Johnson et al. 2003a,b), the energy distributions are characterized by predominantly low energies, with a high energy, non-thermal tail.

For sputtering of both H_2O and O_2 the energy distribution is very sensitive to the incident ion type, energy and surface temperature. For incident heavy ions, O_2 are ejected from the surface according to a measured energy distribution (Johnson *et al.* 1983)

$$F^{surface}(E) \sim \frac{U}{(E+U)^2}, \qquad U = 0.015 \;\; eV, \tag{1a}$$

For an O_2 escape energy of 0.67 eV the direct escape is very small. A distribution of the form

$$F^{surface}(E) \sim \frac{2EU}{(E+U)^3}, \qquad U = 0.055 \;\; eV, \tag{1b}$$

fits the measurements for heavy keV ion sputtering of H_2O (e.g., Johnson 1990). This distribution gives a direct escape fraction of 0.3. However, the data clearly show that for fast light incident ions, and for higher surface temperatures, the peak shifts to lower energies (e.g., Johnson 1990). If Eq. 1a was used for H_2O, the escape fraction becomes 0.05. Recent laboratory measurements for the sputtering by 200-eV electrons of Na and K deposited on ice (Johnson *et al.* 2002b) give a distribution of the form ~ $CEU^x/(E+U)^{2+x}$ with x and U equal to 0.7 and 0.052 for Na and 0.25 and 0.02 for K, where C is the normalization constant (Johnson *et al.* 2002b). These results are consistent with the trace species being carried off by sputtering of the ice matrix. Therefore, Na, which has a similar mass, also has a similar ejecta energy distribution to that for H_2O. The ejecta energy distribution for Na appears to be consistent with the morphology of the extended component of the observed sodium atmosphere (Leblanc *et al.* 2002).

The UV-photolysis of an icy satellite surface also leads to the ejection of H_2O and O_2 molecules. These ejecta energy distributions are closer to Maxwellian distributions at the mean surface temperature corresponding, roughly, to a 'thermal' surface source of H_2O and O_2 molecules, while sublimation, subsurface out-gassing, and meteoroid impact vaporization are thermal sources of H_2O. Since sputtering, radiolysis, and photolysis occur in a porous regolith, the ejecta energy distributions, such as those in Eq. 1, are partially or fully thermalized by the interaction of the ejected molecules with the volume ice.

For all of the above energy distributions, most of the sputtered molecules return to the surface. Assuming no reactions with the surface, the returning O_2 is immediately (on the time scale of the simulation) desorbed thermally, but we assume that returning H_2O, OH, and O stick to the icy surface with nearly unit efficiency (e.g., Smith and Kay 1997). In the present model O atoms undergo recombination to produce more O_2 as discussed below. Using the energy distributions above, surface sputtering is a non-thermal source of H_2O and O_2 (Johnson *et al.* 1983) and an additional thermalized source of O_2 resulting from atmosphere – icy surface exchange (Johnson *et al.*1982). A mean surface temperature of 100 K is used. In radiolysis H_2 is, of course, also produced at about twice the rate of O_2 at the temperatures of interest and also accompanies the production of peroxide (e.g., Johnson *et al.* 2003b; Cooper *et al.* 2003). Since diffusion of radiolytic H_2 through ice and escape to space is efficient (e.g., Johnson 1990; Johnson et al. 2003b), H_2 distributions in the atmosphere are not modeled here. However, H_2 is clearly an important source of neutrals for the Europa torus as discussed at the end of the paper.

2.3. Interactions

The H_2O and O_2 may be dissociated or ionized by the solar UV photons and the plasma electrons through the following reactions:

$$\begin{aligned} O_2 + h\nu, e_p &\rightarrow O(^3P) + O(^3P,^1D,^1S) + e_s + \Delta E_{O2}^{dis} \\ H_2O + h\nu, e_p &\rightarrow \begin{cases} OH + H + e_s + \Delta E_{H2O}^{dis} \\ H_2 + O(^1D) + e_s + \Delta E_{H2O}^{dis} \end{cases} \end{aligned} \quad (2)$$

$$
\begin{aligned}
&O_2 + h\nu, e_p \rightarrow O^+(^4S) + O(^3P,^1D,^1S) + e + e_s + \Delta E_{O2}^{dis-i} \\
&H_2O + h\nu, e_p \rightarrow \begin{cases} OH + H^+ + e + e_s + \Delta E_{H2O}^{dis-i} \\ H + OH^+ + e + e_s + \Delta E_{H2O}^{dis-i} \\ H_2 + O^+ + e + e_s + \Delta E_{H2O}^{dis-i} \end{cases}
\end{aligned} \tag{3}
$$

$$
\begin{aligned}
&O_2 + h\nu, e_p \rightarrow O_2^+ + e + e_s \\
&H_2O + h\nu, e_p \rightarrow H_2O^+ + e + e_s
\end{aligned} \tag{4}
$$

The dissociation and ionization processes lead to the formation of O atoms and OH radicals with excess kinetic energy up to a few eV, determined by the energy release in dissociation (ΔE_{O2}^{dis}, ΔE_{H2O}^{dis}) and dissociative ionization (ΔE_{O2}^{dis-i}, ΔE_{H2O}^{dis-i}) processes. Based on the Bagenal (1994) model of the magnetospheric plasma, two populations of magnetospheric electrons - thermal (with density of 38 cm^{-3} and temperature of 20 eV) and hot (with density of 2 cm^{-3} and temperature of 250 eV) fractions, are taken into account in our model. The EUVAC solar flux model (Richards *et al.* 1994), scaled from Earth to the heliocentric orbit of Jupiter, and the standard set of photoabsorption and electron impact cross sections are used. Because the atmosphere is thin, the calculated photo-ionization and dissociation frequencies are found to be nearly constant with height (Shematovich and Johnson 2001). Although Saur *et al.* (1998) earlier showed that the electron density and temperature changed due to the interaction of the plasma with the ionosphere, they found that the net energy flux of the plasma through the atmosphere did not change greatly. Here we treat the plasma energy flux through the atmosphere to the surface as a constant and use the rates associated with the plasma upstream for comparison to the photo-processes. Any O or OH produced by dissociation is tracked and either escapes or sticks to the surface. We assume that O atoms recombine on the surface forming O_2. The ions formed are assumed to be lost immediately by pickup on planetary magnetic field lines moving at speeds ~ 100 km/s for full corotation past Europa and ~ 20 km/s for field lines in contact with Europa's ionosphere (Paranicas *et al.* 1998, Saur *et al.* 1998). Although some ions produced immediately upstream of Europa may reenter the atmosphere, the rest move away from Europa, gyrating north and south along the local field lines, and are swept far downstream during latitudinal bounce motion along these lines.

Finally, we use the data of Bagenal (1994) to estimate the plasma bombardment rate of the surface-bounded atmosphere. Whereas the energetic ions (measured by the Galileo EPD; e.g., Cooper *et al.* 2001) for the most part pass through this thin atmosphere without collisions, the low energy plasma does not. Therefore, it can remove (sputter) the atmosphere (Johnson 1990, 1994) through the momentum transfer, dissociation, ionization, and charge transfer processes

$$O_2 + p, O^+, S^+, ... \rightarrow \begin{cases} p, O^+, S^+, ... + O_2^* \rightarrow O^* + O^* + \Delta E_{O2}^{dis} \\ p, O^+, S^+, ... + O_2^+ + e \\ H, O, S, ... + O_2^+ \end{cases} \quad (5)$$

$$H_2O + p, O^+, S^+, ... \rightarrow \begin{cases} p, O^+, S^+, ... + H_2^* O \rightarrow OH^* + H + \Delta E_{H2O}^{dis} \\ p, O^+, S^+, ... + H_2O^+ + e \\ H, O, S, ... + H_2O^+ \end{cases} .$$

Momentum transfer and dissociation collisions with energetic magnetospheric ions transfer kinetic energy to H_2O and O_2 gas and form fresh suprathermal O atoms and OH radicals. Hydrogen atoms and molecules formed in H_2O dissociation escape easily from Europa's gravity and are immediately lost to space. Energy input to other species in Europa's atmosphere causes additional atmospheric loss. Saur *et al.* (1998) used an approximate model of atmospheric sputtering and found that these energy inputs drive the dominant loss process. For a convective Maxwellian distribution of the corotating magnetospheric O^+ ions we used parameters close to those of Bagenal (1994) with characteristic ion energy 0.75 keV, mean ion energy 1.5 keV, and flux ~ 1. $\times 10^8$ ions $cm^{-2}\ s^{-1}$. In these calculations we use the collisional momentum transfer and collisional dissociation cross sections from Johnson *et al.* (2002a). A molecular dynamics code was used along with semi-empirical pair potentials to determine the transfer of energy to the motion of the center of mass in $O + O_2$ and $O + H_2O$ collisions. In addition, the internal excitation energy of each molecule was determined as well as the probability of dissociation. These were used to calculate the exit speeds of each molecule or its fragments after a collision.

3. NUMERICAL MODEL

The gas flow in the atmospheric near-surface boundary layer of Europa is strongly non-equilibrium due to three effects:
- nonthermal surface sources of O_2 and H_2O molecules;
-O atoms and OH radicals are formed with suprathermal kinetic energies in the dissociation processes;
-momentum transfer and dissociation collisions by the low-energy magnetospheric plasma ions cause heating and escape, collectively referred to as atmospheric sputtering (Johnson 1994).

Consequently the gas flow in the Europa's surface-bounded atmosphere is described by the following set of kinetic Boltzmann equations for all species

$$\begin{cases} \boldsymbol{v} \dfrac{\partial}{\partial \boldsymbol{r}} f_i + g \dfrac{\partial}{\partial \boldsymbol{v}} f_i = Q_i^{hot} + L_i^{photo} + \sum_j \sum_m J_m(f_i, f_j) \\ \boldsymbol{v} \dfrac{\partial}{\partial \boldsymbol{r}} f_{O+} + g \dfrac{\partial}{\partial \boldsymbol{v}} f_{O+} = \sum_j \sum_m J_m(f_{O+}, f_j) \\ i = O, O_2, H_2O, OH; \quad j = i, O^+ \end{cases} \quad (6)$$

Here the $f_i(\boldsymbol{r},\boldsymbol{v})$ are the distribution functions for j = O, O_2, H_2O, OH, O^+ by translational and internal degrees of freedom; $\boldsymbol{g}$ - is the gravitational acceleration at Europa; Q^{hot} and L^{photo} are source and loss functions for O, OH, O_2, and H_2O in the photolytic and electron impact processes; J_m are the collision terms for elastic, inelastic, dissociation, ionization, and charge transfer collisions (Shematovich *et al.* 1994). The O_2 and H_2O source terms due to surface sputtering and evaporation are taken into account through surface boundary conditions.

This system of kinetic Boltzmann equations is non-linear and the steady-state solutions are computed using the DSMC method (Bird 1994). This approach has been previously used by us to study the hot planetary and satellite coronas (Shematovich *et al.* 1994; Shematovich and Johnson 2001; Shematovich *et al.* 2003). Representative atoms and molecules ejected from the surface, or formed in the atmosphere, are tracked between collisions, and a stochastic scheme is used to choose the position, type and outcome of the next collision. At the top of the atmosphere those atoms or molecules with sufficient energy to escape are removed and the others are computationally reflected. With this numerical model we obtain the velocity distribution functions of the atomic and molecular species, and consequently, the altitude distributions for atmospheric density, temperature, and escape flux.

4. RESULTS

4.1. Surface sources

There are clear hemispherical differences in the amount and nature of the bonding of water molecules on Europa affecting both sublimation and sputtering of water molecules and the production of oxygen from ice. A 1-D model cannot account for these spatial differences, nor can it account for the spatial variation in surface temperature or ion flux. Therefore, this is a parametric study in which the source rates are varied. Earlier we studied the cases for which O_2 was the dominant ejecta. Here we repeat those calculations obtaining a surface source rate of $\sim 2\times10^9$ O_2 $cm^{-2}s^{-1}$ as discussed below. We also modeled the role of water molecules in Europa's atmosphere in a simple way. We are particularly interested here in the relative contributions of thermal versus non-thermal surface processes. In the present study we use O_2 and H_2O sublimation plus sputtering rates of either one or ten times the O_2 flux above. The models considered in this paper are listed in Table I.

[Table I]

In these models the following descriptions are used:

- '**a09'** indicates that O_2 molecules are ejected non-thermally due to surface radiolysis and sputtering by high-energy magnetospheric ions. Their kinetic energies are distributed according to the spectrum of Eq.1a, and the surface flux is equal to 2×10^9 $cm^{-2}s^{-1}$;
- '**b09'** indicates that H_2O molecules are ejected non-thermally due to surface sputtering by high-energy magnetospheric ions. The kinetic energies of these molecules are distributed according to the spectrum of Eq. 1b, and the surface flux is equal to 2×10^9 $cm^{-2}s^{-1}$;

- '**e09'** indicates that O_2 and/or H_2O molecules are ejected thermally due to thermal desorption, photo-desorption, and equilibration in the regolith. These ejecta have a simple Maxwellian distribution for an assumed surface temperature of 100 K, and the surface flux is equal to 2×10^9 $cm^{-2}s^{-1}$**;**
- '**ae09' ('be09')** indicates that O_2 (H_2O) molecules are ejected both thermally (50%) and nonthermally (50%) with the surface flux equal to 2×10^9 $cm^{-2}s^{-1}$.

Models A-C correspond to the pure oxygen surface sources, and Models D-F – to the mixed oxygen and water surface sources. Models in which the surface source flux of O_2 (H_2O) is increased to 2 $x10^{10}cm^{-2}s^{-1}$ with no changes in other parameters for each case were considered as sensitivity studies, but could represent cases for which the local surface is very volatile due to the ice structure or composition. Such large sources of O_2 would require diffusion from depth in the regolith. In addition, the O_2 in the atmosphere is somewhat insensitive to the difference between thermal and non-thermal distributions because of the repeated interactions of O_2 with the surface. Models D-F are likely closer to the globally averaged atmosphere. One can roughly scale these results for other surface source rates because the coupling between the H_2O and O_2 products is weak. However, it is clear from the results given here that a 3-D atmospheric model, accounting for differences in source regions, is needed to correctly describe Europa's atmosphere.

In all models the atmospheric sputtering by low-energy plasma, solar UV and the magnetospheric electron impact dissociation and ionization, were taken into account with the calculated ionization and dissociation frequencies given in the Table II.
[Table II]

4.2. Pure O_2 atmosphere

We first repeated the calculations of the models that were discussed in our previous paper (Shematovich and Johnson, 2001) in order to correct the estimate of surface source rate and clarify the effect of photo-dissociation. The characteristics of atmospheric gas flow in the near-surface region of Europa's atmosphere are given in Figs. 1 and 2 for models with a pure O_2 surface source – Model A (without photo-dissociation), Model B (with photo-dissociation), and Model C (with surface source 10 times higher). In Table IIIa are also given the column densities and total escape fluxes for all pure oxygen models.
[figure 1, figure 2]
In Fig. 1 the height profiles of number (top panel) and column (middle panel) densities, and total escape fluxes (bottom panel) of molecular (solid lines) and atomic (dashed lines) oxygen are given for Models A, B, and C. These densities vs. altitude are not well described by the density vs. altitude profile for a simple out-flowing atmosphere assumed in Saur *et al.* (1998). In the middle panel the range of O_2 column densities in Europa´s atmosphere inferred from HST observations (Hall *et al.*, 1998) is shown by the vertical (dot-dot-dot-dashed) lines. Model column densities were calculated from the top of the neutral atmosphere (here ~700 km). Figure 2 illustrates the detailed flux balance in the neutral surface-bounded atmosphere for Model B. In the top panel the calculated local fluxes of upward and downward moving O_2 molecules (solid and dotted lines) and the direct escape flux (dashed line) are plotted for the main atmospheric constituent – molecular oxygen. Ionization and sweeping is the dominant loss process and "ionization flux" (dot-dashed line) is given for comparison. The latter is calculated as the neutral species column density multiplied by the corresponding ionization rate from by magnetospheric electrons and solar UV radiation (see

Table I). In the middle panel the same fluxes are given for the O_2 dissociation product – atomic oxygen. In the bottom panel the balance of the total flux of oxygen given as O_2 flux is shown. Vertical lines in all panels shows the surface source influx of O_2 molecules.

[Table IIIa]

It is seen that the O_2 atmosphere of Europa is formed and supported due to both thermal and nonthermal processes. In the near-surface region (≤ 10 km) both nonthermal surface sputtering and thermal desorption play a role in the formation of the density distribution. O_2 molecules ejected into this region with kinetic energies higher than the energy of gravitational binding, can easily escape, therefore the thermally re-desorbed O_2 molecules become the dominant fraction of the near-surface region (≤ 100 km). The momentum transfer collisions with the magnetospheric ions and the suprathermal atomic oxygen formed in the dissociation processes lead to the heating of the molecular oxygen in the most upper atmospheric layers (≥ 100 km) and to the additional loss from the atmosphere. Each of these atmospheric regions can have different height scales. Atomic oxygen is formed in the photo-dissociation process with the mean excess kinetic energy of 0.7 – 1.0 eV. Therefore, these atoms easily escape from the rarefied Europa´s atmosphere. The electron impact dissociation of O_2 molecules is accompanied by the formation of O atoms with kinetic energies only slightly exceeding the temperature of the ambient atmospheric gas and do not lead to significant heating or escape. The O atoms formed by dissociation return to the icy satellite surface where they either react or recombine to O_2. In the models examined here the adsorbed O atoms react with the surface and are presumed to eventually 'recombine' and desorb as O_2.

The height profiles of O_2 column densities in Europa´s atmosphere (calculated, as mentioned above, from the top of atmosphere) indicate that the HST estimated column of about 1×10^{15} O_2 cm^{-2} is accumulated in the near-surface region mainly due to the recycling of thermalized molecular oxygen in the atmosphere-icy surface chemical (surface recombination of atomic oxygen) and physical (O_2 adsorption-desorption) exchange. The recycled fraction is accumulated slowly because the mass flow in the near-surface region is controlled by the processes having very different time scales: fast surface-sputtering O_2 influx with the energy spectrum of Eq.1a, slow O_2 atmosphere-icy surface recycling determined by the surface temperature, and direct escape of O_2 molecules with high kinetic energies. The O_2 surface source influx is balanced by the ionization and dissociation losses due to the magnetospheric electrons and solar UV radiation through the whole surface-bounded atmosphere with the minor input of nonthermal escape due to the atmospheric sputtering.

It is seen that O_2 atmosphere of Europa is a surface-bounded (recycling) atmosphere and that a nonthermal surface-sputtering source rate of 2×10^{9} $cm^{-2}s^{-1}$ is sufficient to support the tenuous gas oxygen envelope of Europa first observed by Hall et al. (1995). In our previous paper (Shematovich and Johnson 2001) similar atmospheric characteristics and dependence on altitude were found. The primary atmospheric loss mechanism was shown to be electron impact ionization and pick-up and not atmospheric sputtering as suggested by Saur *et al.* (1998). In addition, including the photo-dissociation was shown to be critical for obtaining the neutral loss rates. Whereas atmospheric pick-up ions are a direct supply of the Europa plasma torus (Schreier *et al.* 1993), the smaller neutral ejection rate creates a neutral oxygen torus which provides a distributed source of oxygen ions for the jovian magnetosphere at Europa's orbit.

In the subsequent discussion, oxygen 'loss' rate will mean all atmospheric loss processes, including ionization and pick-up. Neutral escape will be used in describing the supply of the neutral torus. There still remains a caveat, as the pick-up of O_2^+ followed by recombination or dissociation is a distributed source of energetic neutral O.

The fact that, for a pure O_2 atmosphere, photo-dissociation is the dominant source of ejected O is initially surprising as electron impact is the dominant dissociation mechanism and was the means by which the O_2 atmosphere was observed (Hall *et al.* 1995). Photo-dissociation is a more important neutral loss process than electron impact dissociation because more energy is released to the fragment O than is the case for electron impact dissociation (Rees 1988; Shematovich *et al.* 1994; 1999). The above results were all confirmed here, as indicated in Table IIIa. However, there was an error in our earlier paper. Although the neutral escape rates reached steady state, in the lowest boxes equilibrium was apparently not achieved as it occurs much more slowly as discussed above. Since this directly affects the exchange with the surface, our previous estimate of the surface source rate required to account of the observations is incorrect. Here we find that the necessary amount using a pure O_2 atmosphere is ~ 2.0 (±1.0) $\times 10^9$ $cm^{-2}s^{-1}$. Fortuitously, this is roughly the same size as that used by Saur *et al.* (1998) although their dominant loss process, atmospheric sputtering, is incorrect and better estimates are now available for the surface source rate.

4.3. Concentrations and temperatures in the near-surface O_2 plus H_2O atmosphere

The characteristics of atmospheric gas flow in the near-surface region of Europa's atmosphere are given in Figs. 3 and 4 versus altitude and in Table IIIb for different H_2O surface sources – non-thermal (Model D), thermal (Model E), and mixed (Model F). The number densities of O_2, H_2O, OH and O and their total escape fluxes are given in Fig. 3 (left and right panels, accordingly) and column densities are presented in Table II; the mean kinetic energies and mean flow velocities of O_2, H_2O, OH and O are given in Fig. 4 (right and left panels, accordingly).

[figure 3, figure 4]

In all cases presented here, as well as in the pure O_2 model studied earlier, the atmosphere is found to be a very tenuous and surface-bounded gaseous envelope with O_2 molecules being the main constituent. This is supplemented by an admixture of H_2O, OH and O and a small component of H_2 and H not considered here. This is the case even for models F and G in which the H_2O source rate is ten times the O_2 source rate. Such a composition was predicted for Europa (Johnson *et al.* 1982) as a consequence of gain and loss processes for the three parent molecules ejected from the surface: H_2, H_2O, and O_2. The light H_2 molecules are lost to the Europan neutral torus because of the relatively weak gravitational field of Europa. On the other hand, the heavier H_2O and O_2 molecules are lost mainly through the non-thermal mechanisms: dissociation and ionization, atmospheric sputtering by the low-energy magnetospheric plasma and non-thermal surface ejection. Returning molecules have species-dependent behavior on contact with Europa's surface. The O_2 molecules stick with very low efficiency and are immediately (on the time scale of the simulation) desorbed thermally, but returning H_2O, OH, and O stick to the grains in the icy regolith with unit efficiency (Smith and Kay 1997).

Atomic oxygen O and hydroxyl OH are formed with suprathermal energies in the dissociation processes of the ejected parent H_2O and O_2 molecules by solar UV radiation. Because the near-surface atmosphere is very rarefied, these suprathermal particles do not efficiently thermalize in collisions with the parent molecules (see their mean kinetic energies in Fig. 4). Thus the

suprathermal products efficiently escape from the atmosphere, as seen by escape fluxes in Fig. 3, or they stick to the icy satellite surface, as seen by the height profiles of mean flow velocities in Fig. 4, which are directed to the surface. Therefore, the concentrations and column densities of O and OH in the surface-bounded atmosphere of Europa are low (Fig. 3) as indicated by the column densities in Table IIIa, and b.

Analysis of the H_2O flow characteristics in our model shows that the H_2O escape flux is due mainly to the high-energy tail of the surface-sputtering source. Molecules ejected with the suprathermal energies very efficiently transfer kinetic energy to the more abundant, near-surface oxygen molecules. The H_2O density distribution in the near-surface region ($\leq$ 50 km) is also strongly affected by the sticking to the icy surface. At higher altitudes the direct escape significantly reduces the H_2O abundance.

[Table IIIb]

The concentration of O_2 in Europa's atmosphere within the near-surface region ($\leq$ 50 km) is determined by all three surface sources: surface-sputtering, surface-evaporation, and recycling of surface-thermalized O_2 molecules. As the main atmospheric constituents, the O_2 molecules are efficiently heated by momentum transfer collisions with the incident plasma, the H_2O molecules ejected from the surface with suprathermal energies, and suprathermal dissociation products. More energetic O_2 is found for all models at higher altitudes (Fig. 4, right panels). However, the density profiles of O_2 (Fig. 3) are similar for all models, so the increased production of energetic O_2 from sputtering is balanced by higher escape rates. In all of these models the rate for the dominant loss process, pick-up ion production, is assumed to be independent of altitude, and details of the thermal distributions for neutrals from different models have little effect on the O_2 density profiles. We also note, as seen in Table IV for model D, that although atmospheric sputtering is a smaller loss process than ionization and pick-up in our models, it can be comparable to or larger than photo-dissociation-induced loss.

4.4. Balance and the energy spectra of upward fluxes

The macroscopic characteristics of composition, dynamics, and energy balance of gas flow in the surface-bounded atmosphere of Europa are presented in Figs. 3 and 4. These were derived from the calculated energy distribution functions (EDFs) for all neutral atmospheric constituents. The EDFs characterize the gas flow on the microscopic level.

In the runs for all models from Table I the statistics on the molecule velocities were stored allowing us to estimate the energy distributions of all species. To analyze the particle distributions in Europa's surface-bounded atmosphere the energy spectra of fluxes of upward moving parent H_2O and O_2 molecules were calculated and are shown in Figs. 5a and 5b for Model D. For comparison the energy spectra of surface-sputtering source functions (Eq. 1a) for O_2 and (Eq. 1b) for H_2O are also shown. The heights of 3.6 km and 100 km were taken as the representative of the near-surface environment and of the upper atmospheric layers where atmospheric sputtering becomes important.

[figure 5a]

In Model D the sources of H_2O and O_2 are both nonthermal (Eqs.1a and 1b). It is seen that in the very near-surface region the upward flux of O_2 molecules is characterized by the Maxwellian core, corresponding to the recycled population of molecules with kinetic energies close to the surface temperature, and by a suprathermal tail formed due to both surface-sputtering and momentum transfer collisions with dissociation products. For H_2O, the energy spectrum of upward moving flux

is determined by the surface-sputtering source spectrum and the Maxwellian core does not form because molecules efficiently stick to the icy satellite surface. We suggest the interesting possibility of spatially resolving the composition of source sites for sputtered molecules with an orbital instrument on JIMO since low-energy neutral spectra of H_2O-like molecules suffer little modification after leaving the surface.

[figure 5b]

The net fluxes of parent molecules H_2O and O_2, and of the dissociation products O and OH, can be used for the analysis of mass balance in Europa's surface-bounded atmosphere. In Fig. 6 the height profiles of upward and downward fluxes of O_2, H_2O, O and OH are shown together with the loss fluxes of escaping molecules and "ionization loss fluxes". The latter are calculated as the column density multiplied by the ionization rate (see, Table II) and can be interpreted as the loss flux due to the ion pickup in the atmosphere. From Fig. 6 it is seen that, as in the all of the models described here, mass balance for molecular oxygen is determined primarily by the ionization by magnetospheric electrons in the near-surface region and by the atmospheric sputtering in the upper atmospheric layers.

[figure 6]

As was mentioned above, most of the ejected molecules return to the surface. Collisions between parent molecules and their dissociation products in the very near-surface region lead to the formation of suprathermal tails in the downward fluxes of parent O_2 and H_2O molecules and of O and OH. The energy spectra of these downward fluxes significantly differ from a convective Maxwellian, especially for dissociation products - O and OH. For example, in case of Model D the impacting O_2, O, H_2O, and OH molecules are characterized by the mean kinetic energies equal to 0.02 eV, 0.66 eV, 0.19 eV, and 0.23 eV, correspondingly. These values are much higher than the mean surface temperature of 100 K (0.0086 eV). Such suprathermal neutrals interacting with the icy surface can potentially initiate chemical change on grain surfaces in the regolith (Johnson 2001; Johnson *et al.* 2003a,b).

4.5. Atmospheric Escape and the Europa's Neutral Torus

As was the case for the observed sodium atmosphere/torus at Europa (Leblanc *et al.* 2002), the loss of atmosphere supplies a neutral and plasma torus (Schreier *et al.* 1993). Since ionization is the dominant oxygen loss process in our model, this implies the oxygen ions are primarily supplied by pick-up from Europa's atmosphere and ionization in the oxygen neutral torus is a smaller supply. Since the neutral molecular hydrogen supply rate is roughly twice the surface source rate for molecular oxygen, hydrogen is likely the dominant source for the Europa neutral torus and ionization of hydrogen in the torus is likely the principal supply of hydrogen ions.

Because oxygen loss in these models is dominated by ionization and pick-up, the calculated neutral oxygen supply rate is much lower than the surface source rate given in Table III a, b, and c for all models. These values were calculated as $Q_n = S_{exo} F_{esc}$, where $S_{exo} = C(R_{Eur} + h_{exo})^2$. If we assume the loss is global, so that $C \approx 4\pi$, then $S_{exo} \approx 3.5 \times 10^{17}$ cm^2 for an exobase height h_{exo} = 100 km. The flux of escaping oxygen atoms was taken as equal to $F_{esc} = 2F_{O2} + F_O + F_{H2O} + F_{OH}$ with data taken from Fig. 3 (right panels) and Table III. We obtained the supply rates in the range of $(1.0\text{-}3.0) \times 10^{26}$ O atoms per second for Models D-G for a globally uniform atmosphere. For an O_2 source rate of $\sim 2 \times 10^9$ cm^2, the H_2 source would be $\sim 4 \times 10^9$ cm^2. If the H_2 escape fraction is near unity (e.g., Johnson 1990) this would result in a supply $\sim 3 \times 10^{27}$ H atoms per sec to the neutral torus primarily as H_2. To understand the relative importance of the various processes in Table IV we give the

atmospheric loss rates for all of the interactions for the pure O_2 surface source rate (Model B) and a model with the mixed H_2O and O_2 nonthermal surface source rates (Model D). For comparison, the loss and gain rates of the model by Saur *et al.* (1998) are also given.

[Table IV]

The total loss rate and energy spectra of escaping neutrals from Europa's atmosphere characterize the supply of oxygen and water product neutrals for the inner Jovian magnetosphere. Combining these with the hydrogen loss gives the source terms for the Europa neutral torus recently observed using the Galileo energetic particle data (Lagg *et al.* 2003) and using the Cassini energetic neutral atom data (Mauk *et al.* 2003). The energy spectra of the escaping H_2O and O_2 are indicated in Figs. 5a and 5b as the contributions to the right of vertical lines on the energy spectra of upward fluxes. A rough estimate of the total number N of neutrals in the trans-Europa gas torus can be made using the balance equation $Q_n = N * L_i$, or $N = S_{exo}\,(2F_{O2}/L_{O2} + F_O/L_O + F_{H2O}/L_{H2O} + F_{OH}/L_{OH})$, where Q_n is the total supply rate (Table III) and L_i are the species loss rates due to the ionization by solar UV radiation and by magnetospheric electrons (Table II). Using these supply and loss rates our estimate of the total number N of oxygen neutrals is $\sim(3.0 - 5.0)\times10^{32}$ O atoms as O, O_2, H_2O, or OH for Models D-F (Table IIIa, and b last row). In each case there is a source of neutral hydrogen at least twice the oxygen surface source rate times the escape fraction as discussed above. The density again would be obtained from the hydrogen ionization rate.

Mauk *et al.* (2003) estimated the total number of neutrals in the Europa gas torus to be in the range of $(4.5 - 9.0)\times10^{33}$ atoms. Preliminary analysis of the Cassini UVIS observations (Hansen *et al.* 2003) suggests lower torus content. Because most of the oxygen is lost by pick-up in these models, the supply of neutral hydrogen is larger and, therefore, H is likely the dominant species in the Europa neutral torus. However, the atmosphere is not likely to be globally uniform as mentioned earlier due to variations in the surface composition and to variations in the charged particle flux to the surface. Since most of the ejecta are molecular, the excess energy on dissociation needs to be accounted for and the interactions occurring in the torus must be treated in correctly modeling the neutral torus.

5. SUMMARY AND CONCLUSIONS

We have presented a collisional Monte Carlo model of Europa's atmosphere in which the sublimation and sputtering sources of H_2O molecules and their molecular fragments are accounted for as well as the adsorption, thermalization and re-emission of condensed O_2, a stable decomposition product of H_2O radiolysis. The very tenuous oxygen atmosphere of Europa originates from a balance between sources from irradiation of the icy satellite surface by solar UV photons and magnetospheric plasma and losses from pick-up ionization and ejection following dissociation or collisions with the low energy plasma ions. Since the incident plasma is primarily responsible for both the supply and loss of oxygen, a dense atmosphere does not accumulate (Johnson et al. 1982). The thin, surface bounded atmosphere calculated is also consistent with a recent model for the extended sodium atmosphere at Europa (Leblanc *et al*. 2002; Johnson *et al.* 2002b).

The surface-bounded atmosphere of Europa is characterized by a hot corona formed due to atmospheric sputtering, by suprathermal radicals entering the regolith that can drive radiolytic chemistry, by a supply of pick-up ions to the plasma torus, and by a supply of neutrals to the Jovian inner magnetosphere producing a neutral gas torus along the Europa's orbit. The calculations

described here show that the chemical composition and structure of the atmosphere is determined by both the water and oxygen photochemistry in the near-surface region and the adsorption-desorption exchange by radiolytic water products with the satellite surface. In these models the principal loss of oxygen is by pick-up ionization and not atmospheric sputtering, as suggested by Saur *et al.* (1998). Their large atmospheric sputtering rate came from using an effective interaction cross section that was much too large. However, to confirm this result an accurate, self-consistent model of the electron temperature and density in Europa's atmosphere is needed. In such a model the observations of Hall *et al.* (1995; 1998) constrain the product of the column density and the electron impact ionization rate (Saur *et al.* 1998). Whereas deflection and cooling of the plasma might increase for the largest surface source rates discussed, dramatic differences are not expected for the standard source O_2 rate which is consistent with that used in Saur *et al.* (1998). We further note that, although electron impact is the dominant atmospheric dissociation process, by comparing models A and B it is seen that photo-dissociation is an important loss process and an important supply of oxygen to the neutral torus in addition to atmospheric sputtering. Depending on the characteristics of the H_2O surface source, direct escape of sputtered water molecules also supplies oxygen-containing species.

The surface flux of oxygen that we found earlier (Shematovich and Johnson 2001), to account for the production of the oxygen emissions observed by HST (Hall *et al.*, 1998), was corrected here. Here we also used the fact that the O_2/ H_2O sputtering yield ratio is larger than that measured for laboratory samples because radiolysis is occurring in a very porous regolith (Johnson *et al.*, 2003a,b). Because ionization is a dominant loss mechanism in this model, the surface-bounded atmosphere of Europa is an important source of heavy pick-up ions that directly supply plasma to the inner magnetosphere of Jupiter. The ejected neutrals that populate the neutral torus are subsequently ionized and are a smaller, distributed source of oxygen containing ions for the Europa plasma torus. Because the dominant loss of oxygen in these models is by ionization and pick-up, which must be balanced by a comparable loss of H_2, we find that the dominant supply of neutrals to the torus is radiolytic production and direct escape of molecular hydrogen. Therefore, if the ionization rates used here are correct, the neutral torus will be dominated by hydrogen and the proton source for the Europa plasma will be a distributed source.

If the atmosphere is indeed globally uniform, then the pick-up ionization rate found here is likely to be too large. In fact, HST observations by McGrath *et al.* (2001) suggest the atmosphere might be non-uniform. Noting that the ice coverage of the surface is indeed non-uniform, a preliminary 2-D model was run for a pure oxygen atmosphere (Wong *et al.* 2001). In this model the source of oxygen was the icy leading hemisphere. In steady state, the differences between the leading and trailing oxygen column density was found to be only about a factor of two because oxygen returns to the surface and desorbs many times before being ionized. Hence, oxygen spreads across the surface of Europa. However, molecular oxygen can react in the regolith, a process ignored here. Even if the possible reactions are inefficient, the surface area in the regolith is many orders of magnitude larger than Europa's geometric surface so that such reactions for oxygen in the porous regolith may in fact be likely. If this is the case a non-uniform oxygen atmosphere can result. Therefore, our model will be expanded to a 3-D model. A goal will be to include the effect of the surface catalytic chemistry and the release of trace amounts of SO_2 and CO_2 that are trapped in the surface ice (Johnson *et al.* 2003a,b).

There is a need for reference models of the Europan atmosphere to aid in planning of future missions to Europa such as the Jupiter Icy Moons Orbiter (JIMO), which could conduct orbital measurements of this moon for several months. Johnson *et al.* (1998) noted that Europa surface composition, among the prime science objectives for JIMO, could be inferred in part from orbital measurements of sputtering products comprising the atmosphere. At an orbital altitude of 100 km the data in Figure 3 give densities of 10^6 to 10^7 cm^{-3} for O_2, and 10^3 to 10^5 cm^{-3} for H_2O, O and OH. Moving to a lower orbit ~ 10 km would increase the O_2 and H_2O densities by an order of magnitude but would negligibly change the O and OH densities. Current techniques for bulk measurements of neutral gas, e.g. as to be utilized by the Cassini Orbiter Ion-Neutral Mass Spectrometer at Titan and other Saturnian moons, have a density threshold ~ 10^4 cm^{-3}, so different techniques may be needed to measure OH and other trace species (Na, Mg, K) originating from Europa's surface. Direct imaging of single, H_2O-like low-energy (~ 10 eV) neutrals sputtered from the Europa surface is a possibility and could provide geologic context for surface composition studies. Although we have not attempted to quantify pick-up ion densities and fluxes in the present model, ion composition measurements are far more sensitive, so that even trace species could be measured in the pickup ion populations downstream from Europa and other Galilean moons. The neutral gas torus that extends around Jupiter at Europa's orbit, as discussed above, provides an extended region for JIMO detection of neutrals and ions originating from Europa.

ACKNOWLEDGEMENTS

This work has been supported at UVA by the NSF Astronomy Program and NASA's Planetary Atmospheres Program, and in the Russian Federation by RFBR Project No.02-02-16087. J. F. Cooper acknowledges continuing support at Raytheon and the Goddard Space Flight Center from contracts NASW-02005, NASW-02037, and NAS5-98156, respectively from NASA's Jovian System Data Analysis, Planetary Atmospheres, and Space Science Data Operations Office programs.

REFERENCES

Bagenal, F. 1994. Empirical model of the Io plasma torus: Voyager measurements. *J. Geophys. Res.* **99**, 11043-11062.

Baragiola, R.A., R. A. Vidal, W. Swendson, J. Schou, D. A. Bahr, and C. L. Atteberry 2003. Sputtering of water ice. *Nucl. Instrum. Methods*, in press.

Bar-Nun, A., G. Herman, M. L. Rappaport, and Yu. Mekler 1985. Ejection of H_2O, O_2, H_2, and H from water ice by 0.5-6 keV H^+ and Ne^+ ion bombardment. *Surf. Sci.* **150**, 143-156.

Bird, G. A. 1994. *Molecular Gas Dynamics and the Direct Simulation of Gas Flows*, Clarendon Press, Oxford, England.

Carlson, R. W., R. E. Johnson, and M. S. Anderson 1999. Sulfuric acid on Europa and the radiolytic sulfur cycle. *Science* **286**, 97-99.

Chyba, C. F. 2000. Energy for microbial life on Europa. *Nature* **403**, 381-382.

Cooper, J. F., R. E. Johnson, B. H. Mauk, and N. Gehrels 2001. Energetic electron and ion irradiation of the icy galilean satellites. *Icarus* **149**, 133-159.

Dominé, F., and P. B. Shepson 2002. Air-snow interactions and atmospheric chemistry. *Science* **297**, 1506-1510.

Eviatar, A., A. Bar-Nun, and M. Podolak 1985. Europan surface phenomena. *Icarus* **61**, 185-191.

Hansen, C.J., D.E. Shemansky, and A.R. Hendrix 2003. Observations of Europa's extended atmosphere and torus: oxygen and discovery of hydrogen. *Bul. Am. Astron. Soc.* **34**, 1703 (abstract).

Hall, D. T., D. F. Strobel, P. D. Feldman, M. A. McGrath, and H. A. Weaver 1995. Detection of an oxygen atmosphere on Jupiter's moon Europa. *Nature* **373**, 677-679.

Hall, D. T., P. D. Feldman, M. A. McGrath, and D. F. Strobel 1998. The far-ultraviolet oxygen airglow of Europa and Ganymede. *Astrophys. J.* **499**, 475-481.

Ip, W.-H. 1996. Europa's oxygen exosphere and its magnetospheric interaction. *Icarus* **120**, 317-325.

Ip, W.-H., D. J. Williams, R. W. McEntire, and B. Mauk 1998. Ion sputtering and surface erosion at Europa. *Geophys. Res. Lett.* **25**, 829-832.

Ip, W.-H., A. Kopp, D. J. Williams, R. W. McEntire, and B. Mauk 2000. Magnetospheric ion sputtering: the case of europa and its surface age. *Adv. Space Res*. **26(11)**, 1649-1652.

Johnson, R. E. 1989. Sputtering of a planetary regolith. *Icarus* **78**, 206-210.

Johnson, R. E. 1990. *Energetic Charged Particle Interaction with Atmospheres and Surfaces*, Springer-Verlag, New York.

Johnson, R. E. 1994. Plasma-induced sputtering of an atmosphere. *Sp. Sci. Rev.* **69**, 215-253.

Johnson, R. E. 1998. Sputtering and desorption from icy surfaces. In *Solar System Ices, Astrophys. Space Sci. Library,* pp. 303-331. WKAP, Dordrecht.

Johnson, R. E. 2001. Surface chemistry in the Jovian magnetosphere radiation environment. In *Chemical Dynamics in Extreme Environments* (R. Dessler, Ed.) *Adv. Ser. in Phys. Chem.* pp. 390-419. World Scientific, Singapore.

Johnson, R. E. 2002. Surface boundary layer atmospheres. In *Atmospheres in the Solar System: Comparative Aeronomy* (M. Mendillo, A. Nagy, J. H. Waite, Eds.) pp. 203-219. Geophys. Monograph, AGU.

Johnson, R. E., L. J. Lanzerotti, and W.L. Brown 1982. Planetary applications of condensed gas sputtering. *Nuclear Instruments and Methods* **198**, 147-157.

Johnson, R. E., J. W. Boring, C. T. Reimann, L. A. Barton, J. W. Sieveka, J. W. Garrett, K. P. Farmer, W. L. Brown, L. J. Lanzerotti 1983. Plasma ion-induced molecular ejection on the Galilean satellites: Energies of the ejected molecules. *Geophys. Res. Lett.* **10**, 892-985.

Johnson, R. E., R. M. Killen, J. H. Waite, and W. S. Lewis 1998. Europa's surface and sputter-produced ionosphere. *Geophys. Res. Lett.* **25**, 3257-3260.

Johnson R. E., M. Liu, and C. Tully 2002a. Collisional dissociation cross sections for O + O_2, CO, O_2 and N + N_2. *Planet. Space Sci.* **50**, 123-128.

Johnson, R.E., F. Leblanc, B.V. Yakshinskiy and T.E. Madey, 2002b. Energy Distributions for Desorption of Sodium and Potassium from Ice: the Na/K ratio at Europa. *Icarus* **156**, 136-142.

Johnson, R. E., R. W. Carlson, J. F. Cooper, C. Paranicas, M. H. Moore, and M.C. Wong 2003a. Radiation effects on the surfaces of the Galilean satellites. In *Jupiter: Satellites, Atmosphere, Magnetosphere* (F. Bagenal, Ed.), Univ. of Arizona Press, in press.

Johnson, R. E., T. I. Quickenden, P. D. Cooper, A. J. McKinley, B. Selby, and C. Freeman 2003b. The production of oxidants in Europa's surface. *Astrobiology* **4, #3** in press.

Jurac, S., R. E. Johnson, and J. D. Richardson 2001. Saturn's E ring and production of of the neutral torus. *Icarus* **149**, 384-396.

Kimmel, G. A., and T. M. Orlando 1995. Low-energy (5 - 120 eV) electron stimulated dissociation of amorphous D_2O ice: D(^{2}S), O(^{3}P), and O(^{1}D) yields and velocity distributions. *Phys. Rev. Lett.* **75**, 2606-2609.

Lagg, A., N. Krupp, J. Woch, and D. J. Williams 2003. In-situ observations of a neutral gas torus at Europa. *Geophys. Res. Lett.* ***30***, 1556, DOI: 10.1029/2003GL017214.

Leblanc, F., R.E. Johnson, and M.E. Brown 2002. Europa's Sodium Atmosphere: an Ocean Source? *Icarus* **159**, 132-144.

Kliore, A. J., D. P. Hinson, F. M. Fraser, A. F. Nagy, and T. E. Cravens 1997. The ionosphere of Europa from Galileo radio occultations. *Science* **227**, 355-358.

Mauk, B. H., D. G. Mitchell, S. M. Krimigis, E. C. Roelof, and C. P. Paranicas 2003. Energetic neutral atoms from a trans-Europa gas torus at Jupiter. *Nature* **421**, 920-922.

McCord, T. B., G. B. Hansen, D. L. Matson, T. V. Johnson, J. K. Crowley, F. P. Fanale, R. W. Carlson, W. D. Smythe, P. D. Martin, C. A. Hibbits, J. C. Granahan, and A. Ocampo 1999. Hydrated salt minerals on Europa's surface from the Galileo near-infrared mapping spectrometer (NIMS) investigation. *J. Geophys. Res.* **104**, 11827-11852.

McGrath, M. A., P. D. Feldman, D. F. Strobel, K. Retherford, B. Wolven, and H. W. Moos 2000. HST/STIS Ultraviolet Imaging of Europa. *Bul. Am. Astron. Soc.* **31**, 1056 (abstract).

Paranicas, C., A. F. Cheng, and D. J. Williams 1998. Inference of Europa's conductance from the Galileo Energetic Particles Detector. *J. Geophys. Res.* **103**, 15001-15007.

Paranicas, C., J. M. Ratliff, B.H. Mauk, C. Cohen, and R. E. Johnson 2002. The ion environment near Europa and its role in surface energetics. *Geophys. Res. Lett.* **29**, 18-1, DOI 10.1029/2001GL014127.

Phillips, C. B., A. S. McEwen, G. V. Hoppes, S. A. Fagents, R. Greeley, J. E. Klemaszewski, R. T. Pappalardo, K. P. Klaasen, and H. H. Breneman 2000. The search for current geologic activity on Europa. *J. Geophys. Res.* **105**, 22579-22597.

Pospieszalska, M. K., and R. E. Johnson 1989. Magnetospheric ion bombardment profiles of satellites - Europa and Dione. *Icarus* **78**, 1-12.

Rees, M.H. 1989. *Physics and chemistry of the upper atmosphere*, Cambridge University Press, Cambridge.

Richards, P. G., J. A. Fenelly, and D. G. Torr 1994. EUVAC: A solar flux model for aeronomic calculations. *J. Geophys. Res.* **99**, 8981-8990.

Saur, J., D. F. Strobel, and F. M. Neubauer 1998. Interaction of the Jovian magnetosphere with Europa: constraints on the atmosphere. *J. Geophys. Res.* **103**, 19947-19962.

Schreier, R., A. Eviator, V. M. Vasiliunas, and J. D. Richardson 1993. Modeling the Europa plasma torus. *J. Geophys. Res.* **98**, 21231-21242.

Shematovich, V. I., and R. E. Johnson 2001. Near-surface oxygen atmosphere at Europa. *Adv. Space Res*. **27**, 1881-1888.

Shematovich, V. I., D. V. Bisikalo, and J.-C. Gerard 1994. A kinetic model of the formation of the hot oxygen geocorona. I. Quiet geomagnetic conditions. *J. Geophys. Res.* **99**, 23217-23226.

Shematovich V.I., J.-C. Gerard, D. V. Bisikalo, and B. Hubert 1999. Thermalization of O(1D) atoms in the thermosphere. *J. Geophys. Res.,* **104**, 4287-4295.

Shematovich, V. I., R. E. Johnson, M. Michael, and J. G. Luhmann 2003. Nitrogen loss from Titan. *J. Geophys. Res.* **108**, 5087, DOI 10.1029/2003JE002094.

Shi, M., R. A. Baragiola, D. E. Grosjean, R. E. Johnson, S. Jurac, and J. Schou 1995. Sputtering of water ice surfaces and the production of extended neutral atmospheres. *J. Geophys. Res.* **100**, 26387-26395.

Smith, R. S., and B. D. Kay 1997. Adsorption, desorption and crystallization kinetics in nanoscale water films. *Recent Res. Devel. Phys. Chem.* **1**, 209-219.

Spencer, J. R., L. K. Tamppari, T. Z. Martin, and L. D. Travis 1999. Temperatures on Europa from Galileo PPR: Nighttime thermal anomalies, Science **284**, 1514–1516.

Strazzulla, G., J. F. Cooper, E. R. Christian, and R. E. Johnson 2003. Ion irradiation of TNOs: from the fluxes measured in space to the laboratory experiments. *Comptes Rendus Physique* **4**, 791-801.

Wong, M. C., R. W. Carlson, and R. E. Johnson 2001. Model simulations for Europa's atmosphere. *Bul. Am. Astron. Soc.* **32**, 1056 (abstract).

Table I.
Calculated models

Model[a,b]	**O_2 surface source rate, [$cm^{-2}s^{-1}$] and energy spectrum**	**H_2O surface source rate, [$cm^{-2}s^{-1}$] and energy spectrum**
A(a09-phd)	2.0×10^9 sputtering Eq. (1a) without photodissociation	- no
B(a09+phd)	2.0×10^9 sputtering Eq. (1a) with photodissociation	- no
C(a10+phd)	2.0×10^{10} sputtering Eq. (1a) with photodissociation	- no
D(a09b09)	2.0×10^9 sputtering Eq. (1a)	2.0×10^9 sputtering Eq. (1b)
E(a09e10)	2.0×10^9 sputtering Eq. (1a)	2.0×10^{10} evaporation with T_{surf}=100K
F(a09be10)	2.0×10^9 sputtering Eq. (1a)	2.0×10^{10} 50% sputtering Eq. (1b) ; 50% evaporation with T_{surf}=100 K

[a] -impact processes by the solar UV radiation with mean level of solar activity and by the magnetospheric plasma with two populations of magnetospheric electrons - thermal (with density of 38 cm^{-3} and temperature of 20 eV) and hot (with density of 2 cm^{-3} and temperature of 250 eV) fractions, were taken into account;

[b] - a convective Maxwellian distribution of the corotating magnetospheric O^+ ions with characteristic ion energy 0.75 keV, mean ion energy 1.5 keV, and flux ~ $1.\times10^8$ ions cm^{-2} s^{-1} was used as a low-energy magnetospheric ion influx into the atmosphere.

Table II.
Dissociation and ionization frequencies for solar UV radiation and magnetospheric electron impact for Europa atmosphere

Process rate, [s^{-1}]	**O_2**	**O**	**H_2O**	**Source**
Photoionization	2.8(-8) 1.9(-8) ----	1.7(-8) 7.8(-9) ----	2.2(-8) 1.5(-8) -----	Models A-H Schreier *et al.* (1993) Saur *et al.* (1998)
Electron impact ionization	1.8(-6) 2.4(-7) 1.9(-6)	1.8(-7) 1.2(-7) ----	2.7(-6) 1.3(-7) -----	Models A-H Schreier *et al.* (1993) Saur *et al.* (1998)
Photodissociation	1.8(-7) 2.4(-9) ----		1.1(-7) 4.5(-7) ----	Models A-H Schreier *et al.* (1993) Saur *et al.* (1998)
Electron impact dissociation	3.4(-7) 2.3(-7) 3.8(-7)		4.1(-6) 4.5(-7) -----	Models A-H Schreier *et al.* (1993) Saur *et al.* (1998)

[a] – $a(b)=a*10^b$

Table IIIa
Characteristics of Gas Flow in the Surface-bounded Atmosphere of Europa

Models	**A(a09-phd)**	**B(a09+phd)**	**C(a10+phd)**
O_2 column density, (cm^{-2})	8.2(14)[a]	1.2(15)	1.3(16)
O column density, (cm^{-2})	2.3(6)	2.4(13)	2.6(14)
O_2 escape flux ($cm^{-2}s^{-1}$) and MKE[b] , (eV)	4.1(6) 3.2	4.0(6) 11.4	4.4(7) 2.9
O escape flux, ($cm^{-2}s^{-1}$) and MKE[b] , (eV)	1.6 (4) 8.1	3.1(8) 0.4	2.5(9) 0.4
Total O atom supply rate, Q_n (s^{-1})[c]	2.9(24)	1.1(26)	9.2(26)
Total number N of oxygen neutrals in the torus	1.6(30)	6.1(32)	5.0(33)

[a] – a(b)=a*10^b;

[b]– mean kinetic energy (MKE) of escaping particles was calculated as ratio of total energy flux to total particle flux of escaping particles minus the escape energy (0.68, and 0.34 eV for O_2, and O, respectively);

[c] – total oxygen atom supply rate to neutral torus assuming global loss through the surface area S_{exc} ≈3.5 x10^{17} cm^2 – see subsection 4.5.

Table IIIb.
Characteristics of Gas Flow in the Surface-bounded Atmosphere of Europa

Models	**D(a09b09)**	**E(a09e10)**	**F(a09be10)**
O_2 column density, (cm^{-2})	7.8(14)[a]	9.3(14)	8.0(14)
H_2O column density, (cm^{-2})	9.2(11)	9.4(11)	4.5(12)
O column density, (cm^{-2})	4.2(12)	2.4(12)	3.9(12)
OH column density, (cm^{-2})	3.0(10)	4.6(09)	5.5(10)
O_2 escape flux, ($cm^{-2}s^{-1}$), and MKE[b] , (eV)	2.5(8) 17.0	2.1(8) 3.3	2.1(8) 16.0
H_2O escape flux, ($cm^{-2}s^{-1}$), and MKE[b] , (eV)	4.3(7) 1.8	7.2(5) 0.3	8.9(7) 1.7
O escape flux, ($cm^{-2}s^{-1}$), and MKE[b] , (eV)	2.4(8) 0.4	2.6(8) 0.4	2.2(8) 0.4
OH escape flux, ($cm^{-2}s^{-1}$), and MKE[b] , (eV)	2.4(4) 0.3	3.2(3) 0.5	3.9(4) 0.4
Total O atom supply rate, Q_n , (s^{-1})[c]	2.6(26)	2.3(26)	2.4(26)
Total number N of oxygen neutrals in the torus	5.3(32)	5.6(32)	4.9(32)

[a] – a(b)=a*10^b;

[b]– mean kinetic energy (MKE) of escaping particles was calculated as ratio of total energy flux to total particle flux of escaping particles minus the escape energy (0.68, and 0.34 eV for O_2, and O, respectively);

[c] – total oxygen atom supply rate to neutral torus assuming global loss through the surface area S_{exc} ≈3.5 x10^{17} cm^2 – see subsection 4.5.

Table IV.
Total loss rates in Europa's atmosphere

Loss process rate, [O_2 mol. s^{-1}]	**Model B(a09)**	**Model D(a09b09)**	**Saur et al. (1998)**
Atmospheric sputtering	4.0(6)*3.5(17)=1.4(24)	2.5(8)*3.5(17)=8.8(25)	7.3(26)
Photo-dissociation	3.2(8)*3.5(17)/2=5.6(25)	2.4(8)*3.5(17)/2=4.2(25)	-----
Ionization	5.4(26)	4.7(26)	1.2(26)
Total gain	1.9(9)*3.1(17)=6.0(26)	1.9(9)*3.1(17)=6.0(26)	8.5(26)
O atom supply rate, [O atoms s^{-1}]	1.2(26)	2.6(26)	1.5(27)

[a] – a(b)=a*10^b.

FIGURE CAPTURES

Figure 1. Height profiles of number density (top panel), column density (middle panel) and total escape flux (bottom panel) of O_2 (solid lines), and O (dashed lines) in the pure O_2 surface-bounded atmosphere of Europa for Models A (thin lines), B (midlines), and C (thick lines). Column densities in the middle panel were calculated from the upper boundary of atmosphere; vertical lines (triple dot-dashed line) in this panel indicate the constraints on the O_2 column density inferred from HST observations (Hall *et al.*, 1998).

Figure 2. Flux balance in the pure O_2 surface-bounded atmosphere of Europa for Model B. In the top panel the O_2 local upward (solid line) and downward (dotted line) fluxes, total escape flux (dashed line) and the local "ionization flux" by magnetospheric electrons (dash-dotted line) are given. In the middle panel the same fluxes for atomic oxygen are shown. In the bottom panel the upward flux (solid line), and total loss flux (dashed line) of O_2 molecules are presented. In all panels the vertical line (triple dot- dashed line) corresponds to the surface O_2 source with the flux equal to 2×10^9 $cm^{-2}s^{-1}$. The local "ionization flux" is equal to the local O_2 column density multiplied by the ionization frequency. Total loss flux is a sum of O_2 and O escape fluxes and of local "ionization flux".

Figure 3. Height profiles of number densities (left panels) and total escape fluxes (right panels) of O_2 (solid line), H_2O (dot-dashed line), OH (dot-dot-dot-dashed line) and O (dashed line) in the surface-bounded atmosphere of Europa for Models D (top panels), E (middle panels), and F (bottom panels). Dotted line in right hand panels is the O_2 source rate.

Figure 4. Height profiles of mean velocity (left panels) and mean kinetic energy (right panels) of O_2 (solid line), H_2O (dot-dashed line), OH (dot-dot-dot-dashed line) and O (dashed line) in the surface-bounded atmosphere of Europa for Models D (top panels), E (middle panels), and F (bottom panels).

Figure 5a. Energy spectra (solid lines) of upward fluxes of O_2 and H_2O in the near-surface region at height of 3.6 km for Model D. Energy spectra (1a) an (1b) of surface sources are shown by dashed lines. Vertical dot-dot-dot-dashed lines at 0.38 eV and 0.67 eV show the escape energy of H_2O and O_2 molecules.

Figure 5b. Same as Figure 6a, but at height of 100 km.

Figure 6. Flux balance in the mixed O_2 and H_2O surface-bounded atmosphere of Europa for Model D. Left panels show the fluxes of O_2 and O, and right panels - fluxes of H_2O, and OH. Line styles for both left and right panels are the same as ones in Figure 2.

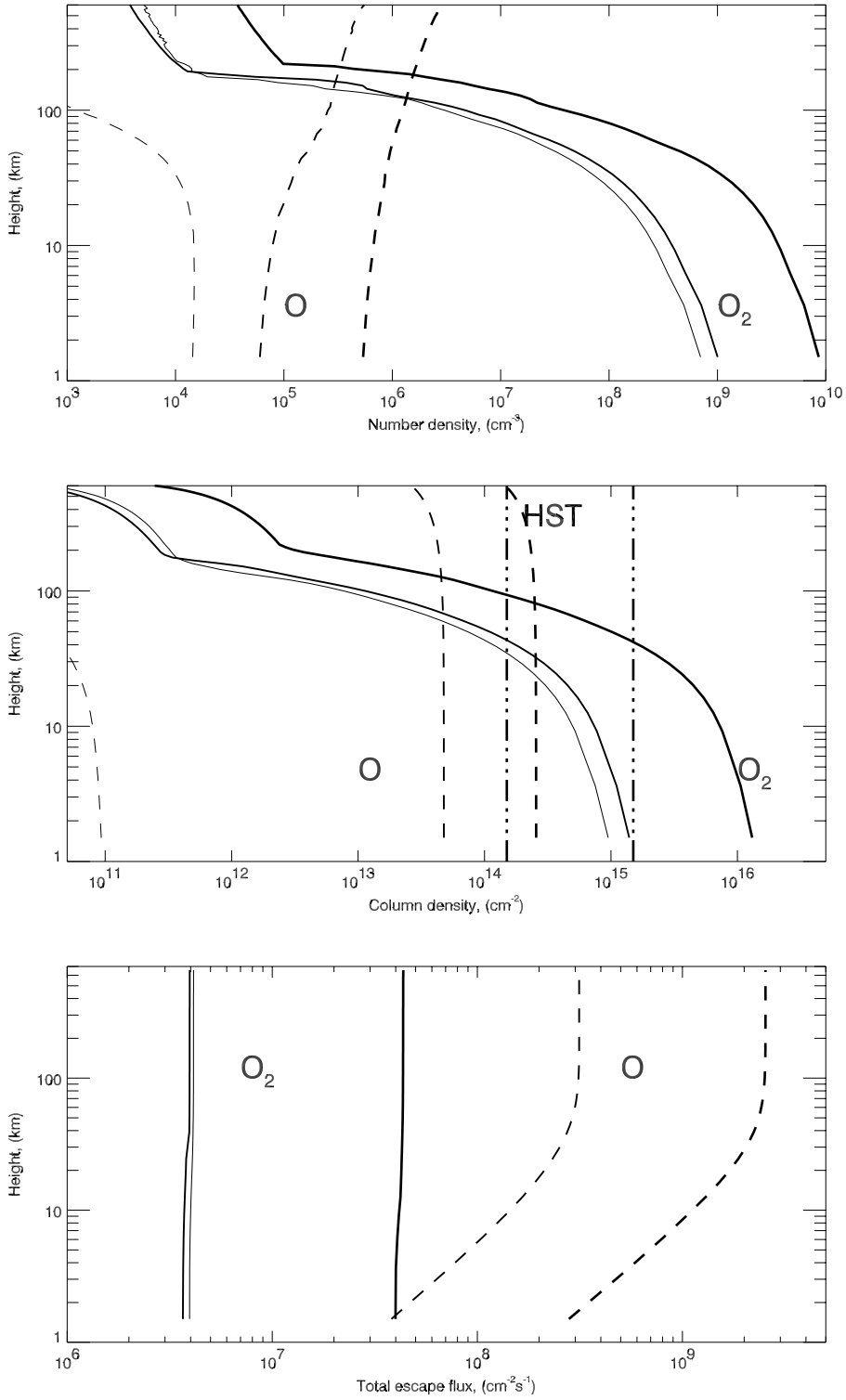

Figure 1, Shematovich et al., Surface-bounded atmosphere of Europa

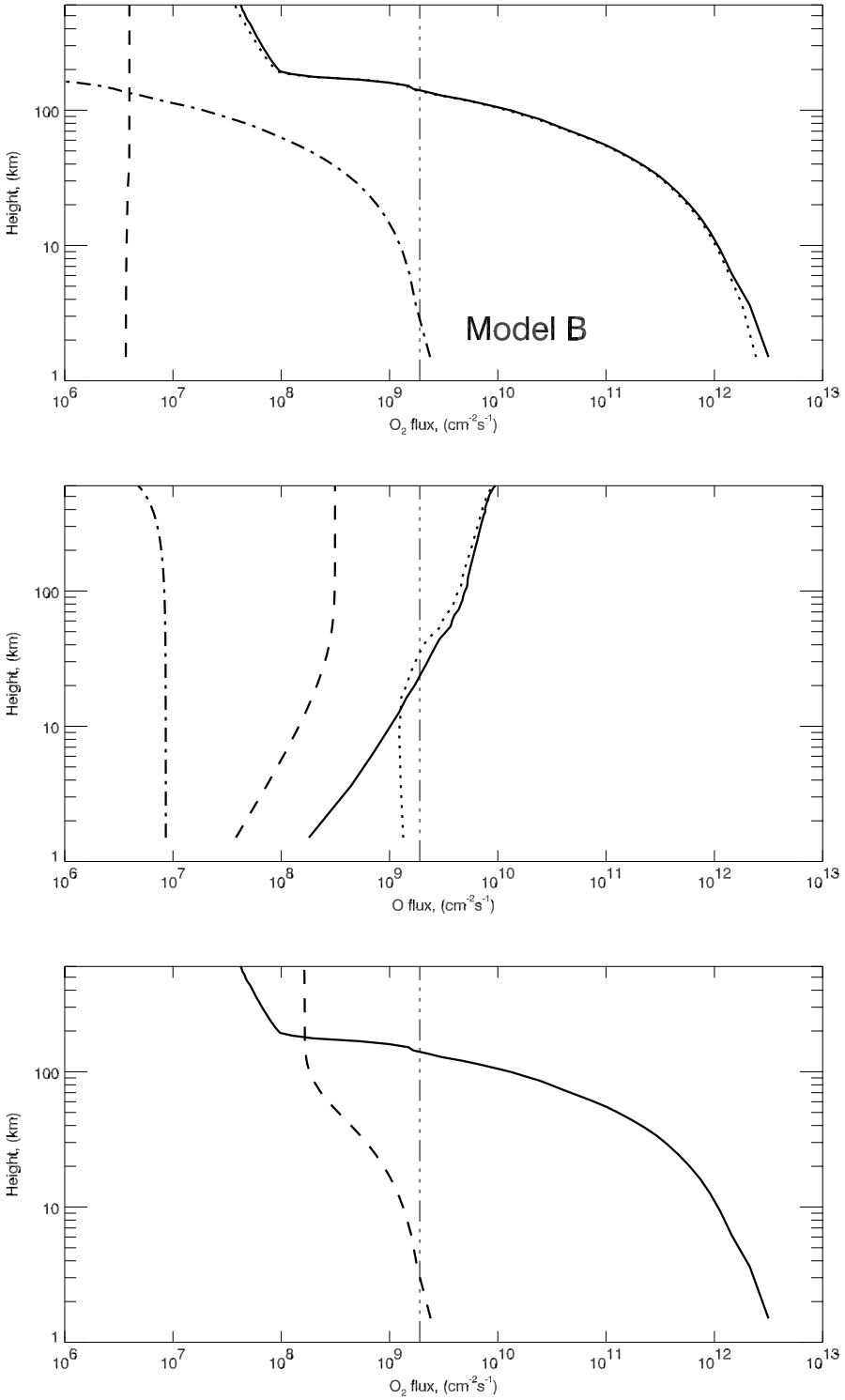

Figure 2, Shematovich et al., Surface-bounded atmosphere of Europa

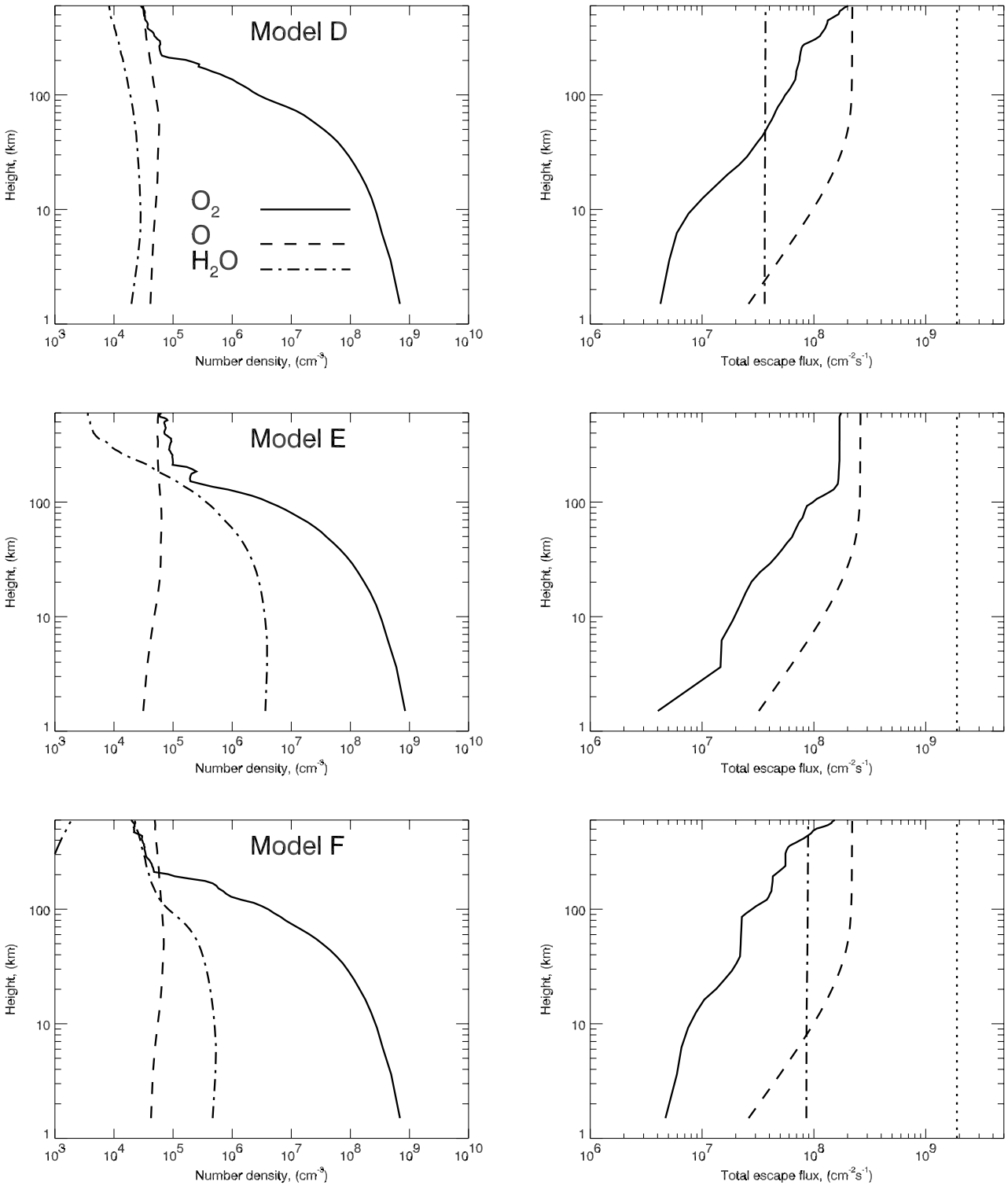

Figure 3, Shematovich et al., Surface-bounded atmosphere of Europa

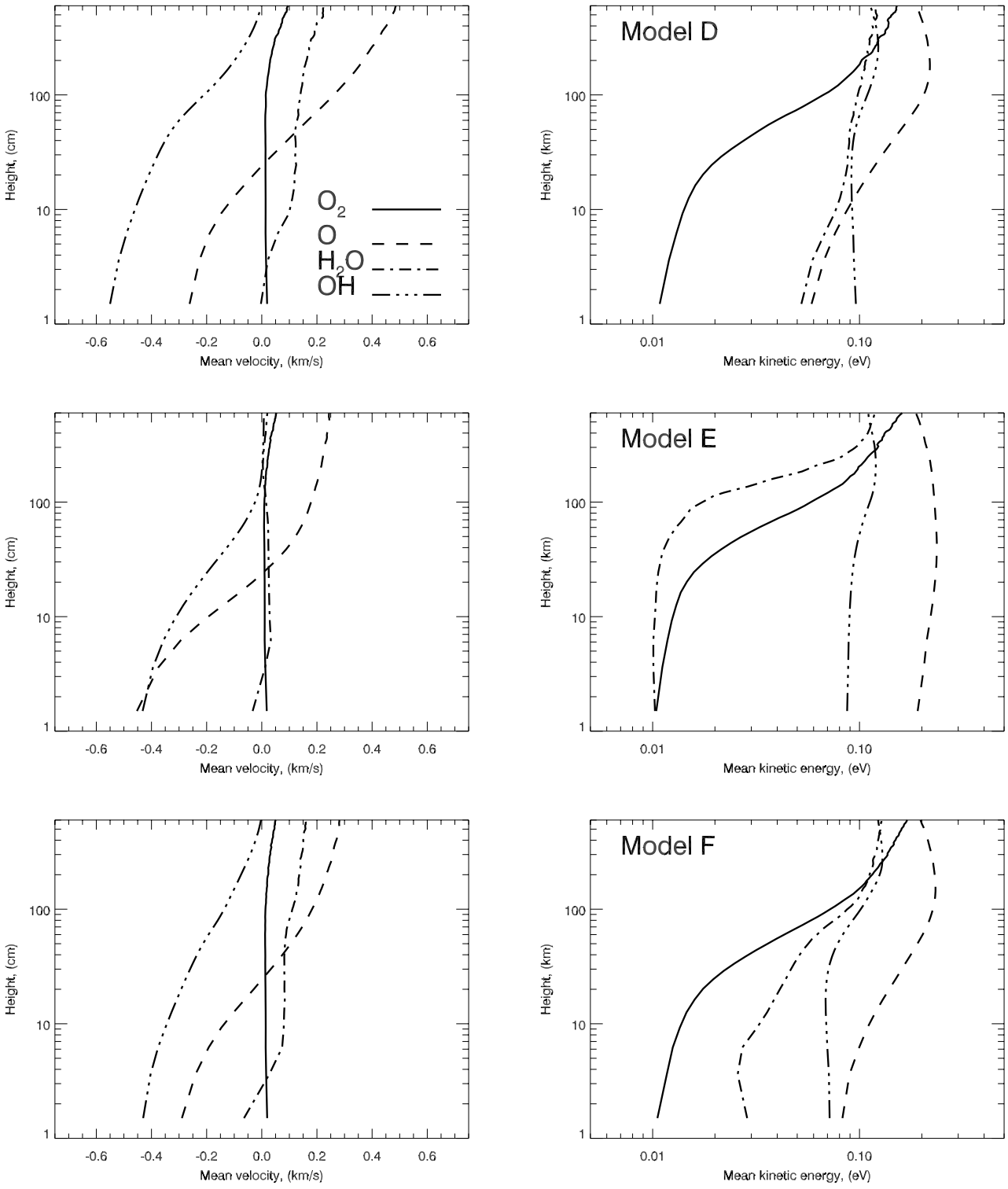

Figure 4, Shematovich et al., Surface-bounded atmosphere of Europa

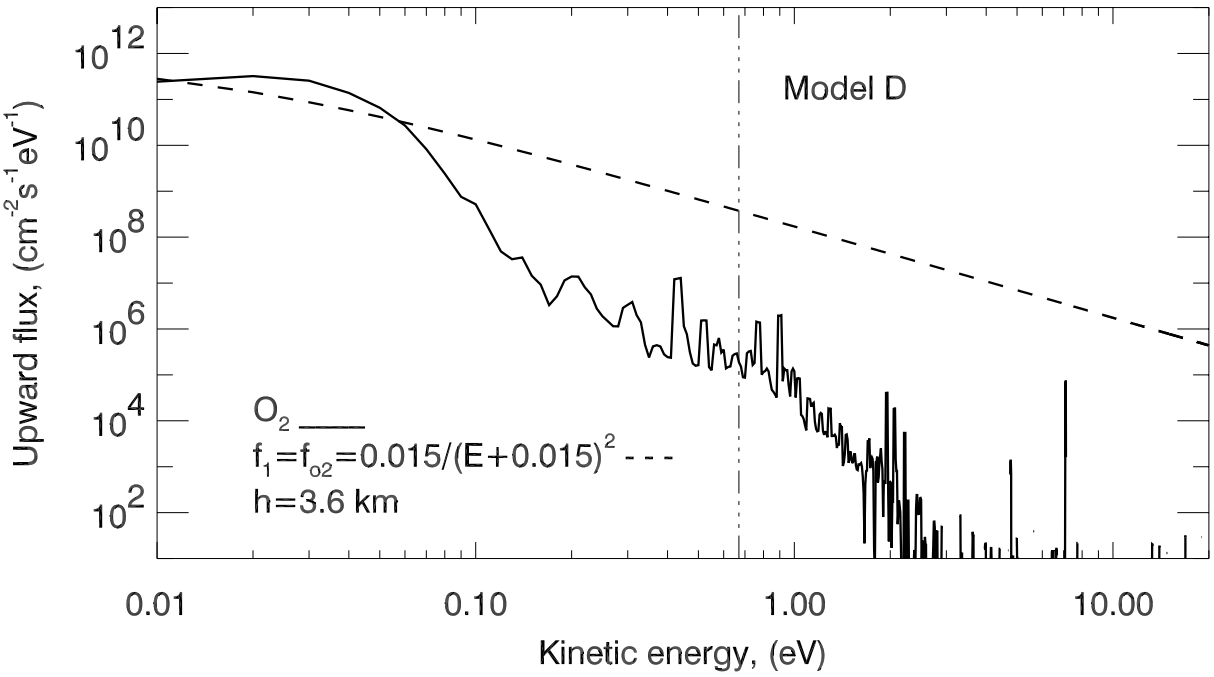

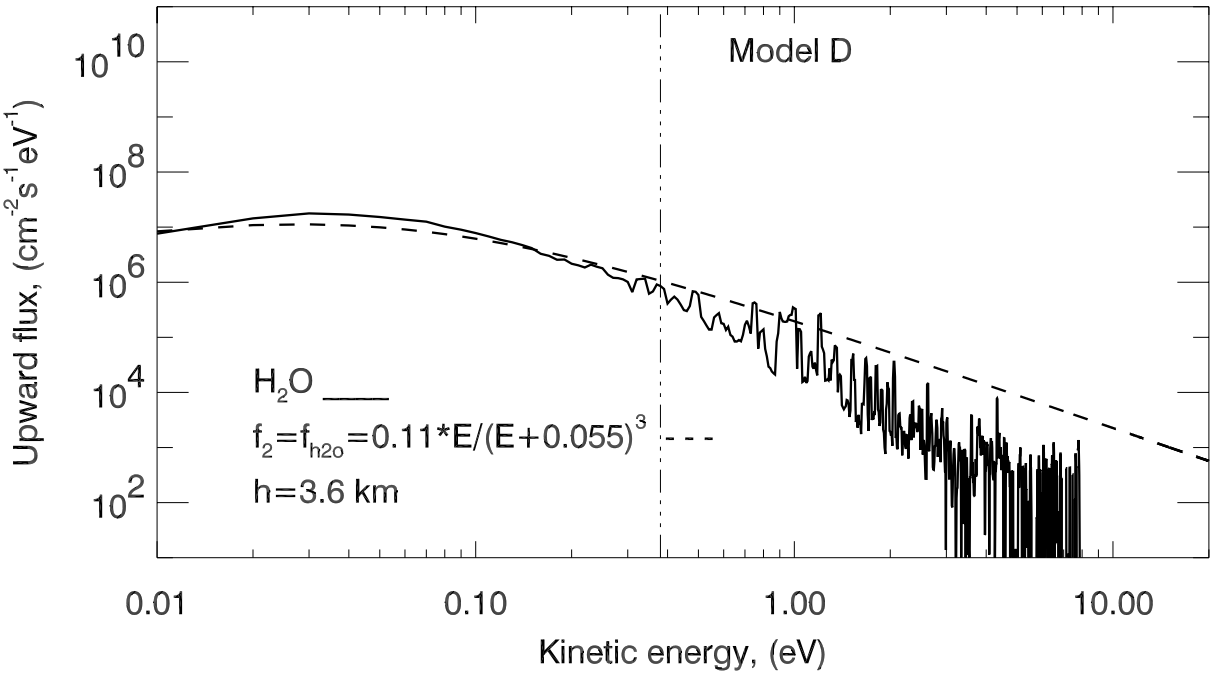

Figure 5a, Shematovich et al., Surface-bounded atmosphere of Europa

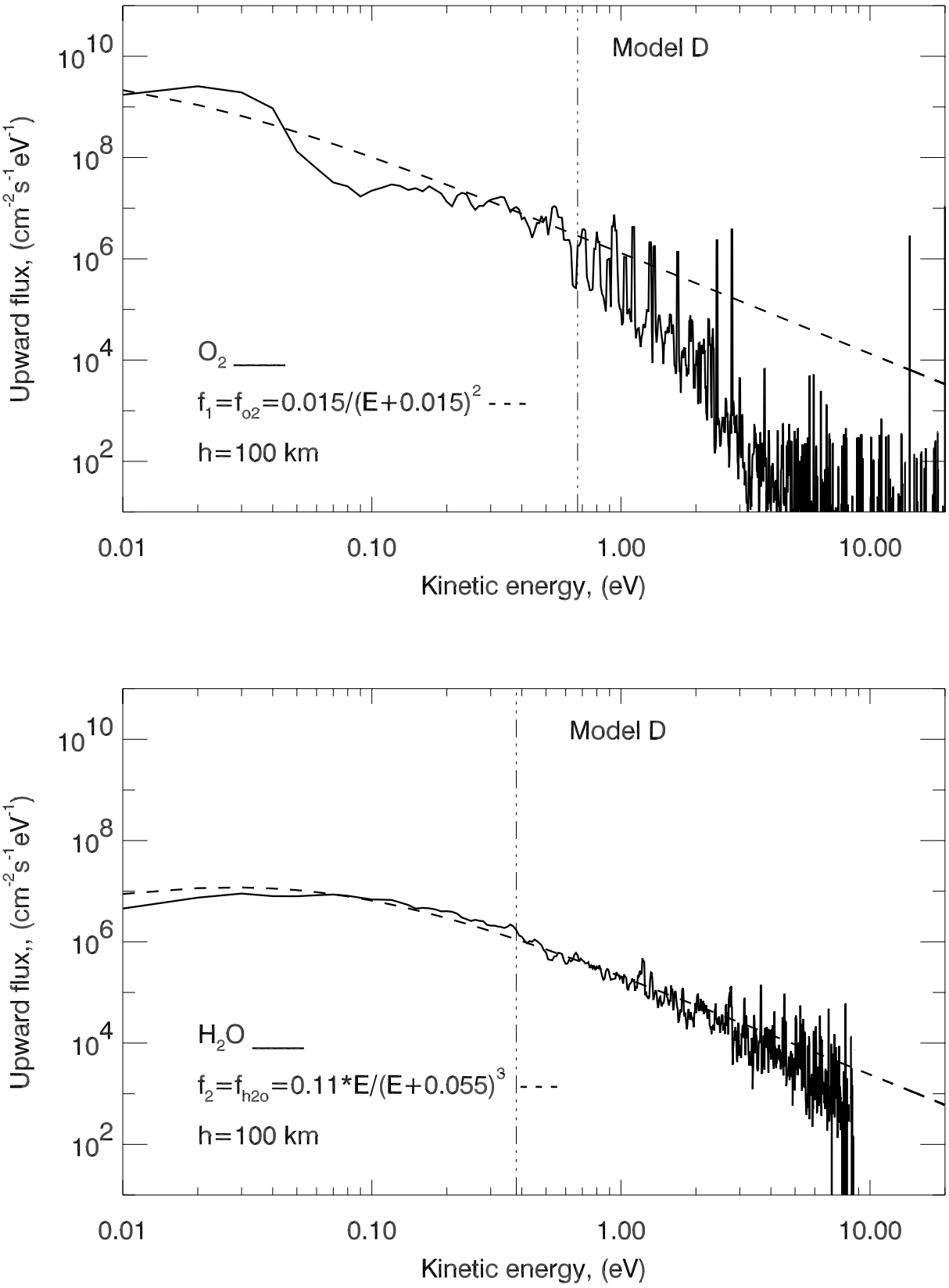

Figure 5b, Shematovich et al., Surface-bounded atmosphere of Europa

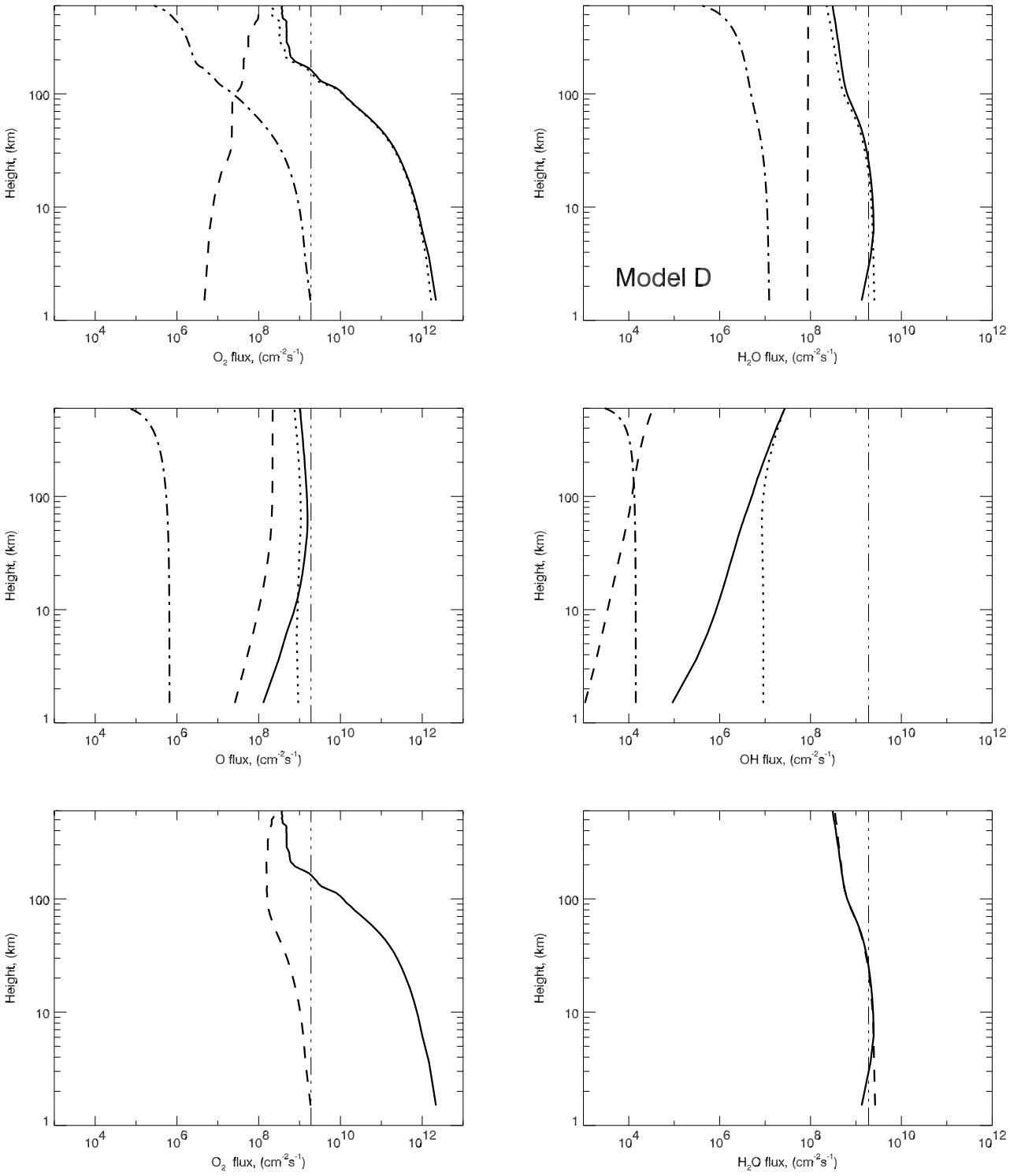

Figure 6, Shematovich et al., Surface-bounded atmosphere of Europa